Sensors & Actuators: B. Chemical 343 (2021) 130173

Contents lists available at ScienceDirect

Sensors and Actuators: B. Chemical

journal homepage: www.elsevier.com/locate/snb

Tailoring properties of indium tin oxide thin films for their work in both electrochemical and optical label-free sensing systems

P. Sezemsky [a], D. Burnat [b], J. Kratochvil [a], H. Wulff [c], A. Kruth [d], K. Lechowicz [b], M. Janik [b,e], R. Bogdanowicz [e], M. Cada [f], Z. Hubicka [f], P. Niedziałkowski [g], W. Białobrzeska [g], V. Stranak [a], M. Śmietana [b,*]

[a] University of South Bohemia, Branisovska 31, 37005, Ceske Budejovice, Czech Republic
[b] Warsaw University of Technology, Institute of Microelectronics and Optoelectronics, Koszykowa 75, 00-662, Warsaw, Poland
[c] University of Greifswald, Felix-Hausdorff-Str. 6, 17489, Greifswald, Germany
[d] INP Greifswald e.V., Felix-Hausdorff-Straße 2, 17489, Greifswald, Germany
[e] Gdansk University of Technology, Narutowicza 11/12, 80-233, Gdansk, Poland
[f] Academy of Science of the Czech Republic, Na Slovance 2, 18221, Prague, Czech Republic
[g] University of Gdansk, Wita Stwosza 63, 80-308, Gdansk, Poland

ARTICLE INFO

Keywords:
Label-free sensing
Indium tin oxide
Thin film properties
Optical fiber sensors
Electrochemistry
Lossy-mode resonance
Biosensing

ABSTRACT

This work is devoted to the identification properties of indium tin oxide (ITO) thin films responsible for their possible application in combined optical and electrochemical label-free sensing systems offering enhanced functionalities. Since any post-processing would make it difficult to identify direct relation between deposition parameters and properties of the ITO films, especially when deposition on temperature-sensitive substrates is considered, the films were deposited using reactive high power impulse magnetron sputtering (HiPIMS) at low temperature and with no post-deposition annealing. We focused mainly on the impact of reactive gases, such as oxygen or nitrogen introduced to the process chamber, on control over plasma parameters and subsequently properties of the films. The properties of the films were investigated using X-ray diffractometry, spectroscopic ellipsometry, four-point probe, and cyclic voltammetry. For presenting optical sensing capabilities, the tailored ITO films in addition to silicon and glass wafers were also deposited on the core of optical fibers to induce the lossy-mode resonance (LMR) phenomenon. The existence of specific deposition conditions resulting in ITO film properties offering both high-quality electrochemical and LMR responses has been experimentally proven. It has been found that the crystalline structure of ITO plays a key role in the determination of both the sensing capabilities. Finally, label-free sensing of antibody-antibody interactions in both optical and electrochemical domains for the sensor with tailored ITO film has been shown.

1. Introduction

Optical sensors, especially those based on optical fibers, have been under intensive development for the last 30 years [1]. Significant progress has been made for the sensors used in medicine, defense and security, aerospace application, as well as many others [2]. They are small in size, offer rapid response, make low-cost fabrication possible, as well as are resistant to electromagnetic interference. There is a large variety of optical fiber sensing concepts [1], where those based on the devices coated with thin films are of particular interest due to their capability for large-scale fabrication. Among other thin-film-based optical phenomena, a lossy-mode resonance (LMR) can be found [3]. The LMR sensors may offer exceptionally high sensitivity to change in optical properties at their surface what next to surface plasmon resonance (SPR) sensors, makes them very promising for label-free chemical and biological sensing [4]. To obtain the LMR, the film must be thick enough and the real part of the electrical permittivity of the film must be positive and higher in magnitude than both its imaginary part and the permittivity of the surrounding medium [5,6]. Since electrical permittivity is correlated with refractive index (RI), the properties of the LMR depend on optical properties of the thin film and these mainly influence the RI sensitivity of the devices [5]. Changes in properties of the films, as

* Corresponding author.
E-mail address: M.Smietana@elka.pw.edu.pl (M. Śmietana).

https://doi.org/10.1016/j.snb.2021.130173
Received 8 January 2021; Received in revised form 22 May 2021; Accepted 24 May 2021
Available online 26 May 2021

well as properties of the external medium, modify the resonant conditions resulting in the shift of the LMR wavelength observed in transmission spectrum $T(\lambda)$ of the optical fiber device. It has been clearly shown that the sensitivity, quality of the LMR, and the RI of the film are strongly correlated [3,7]. Thus, when fabricating optical sensors, especially those based on the LMR effect, real (n) as well as the imaginary part of RI (k) are crucial parameters determining their performance.

The LMR effect, described for the first time in 1993 [8], was implemented for sensing purposes in 2005 when silicon was used as a thin film material for coating of the optical fiber core [9]. Later on, also an application of other materials such as SnO_2 [10], ZnO [11,12], TiO_2 [13,14], DLC [15], SiN_x [16], HfO_2, ZrO_2, Ta_xO_y [17], as well as various polymers [5,18,19] for receiving LMR has been reported. It must be noted that deposition of these films is significantly more cost-effective than deposition of gold, which is typically required of achieving the SPR effect. Among other LMR structures can be also found those based on indium tin oxide (ITO) thin films deposited on fused silica glass [20]. ITO has been used as a perspective coating for LMR-based optical fiber sensors where it provides high RI sensitivity [21]. Due to the sensitivity, especially to RI changes in the proximity of the thin film surface, when biofunctionalized ITO-coated optical fiber LMR label-free biosensors of immunoglobulin [22] and thrombin [23] have been reported. Furthermore, ITO may also offer low electrical resistivity [24,25] and suitable bandgap for application as an active electrode for initiating electrochemical processes [26,27]. In this case, changes in charge transfer at the sensor surface are monitored and widely used for label-free sensing purposes too [28]. Hence, optical fiber structures coated with tailored in properties ITO thin film offer a great opportunity to combine optical, in particular LMR, and electrochemical sensing techniques [29,30], i.e. it offers a possibility of application two independent sensor interrogation methods in the same place and time [31]. Such an approach may offer cross-verification of the readouts and an extended sensing range. Moreover, the combined technique makes possible electrochemical processing of surface, such as electrochemical biofunctionalization, that can be followed by optical detection [32]. The concept of electrochemically-enhanced optical sensing has already been reported in our former works for successful detection of ketoprofen [33], isatin [31], and also label-free biosensing [34,32]. Moreover, we have also shown that properties of ITO highly depend on deposition conditions what makes them suitable for LMR-based or electrochemical sensing, but rarely for the combined approach [29].

There are various techniques already applied for ITO thin film deposition, such as e.g., pulsed laser deposition [35], vacuum thermal evaporation [36], dip-coating wet chemistry [37], and layer-by-layer deposition [13]. Among them, an application of magnetron sputtering is of particular interest due to the possibility of precise tailoring of the film properties as demonstrated for highly sensitive SnO_2-LMR sensors [38]. However, in cases of ITO deposition on thermally sensitive substrates, where the post-deposition annealing step cannot be performed, a conventional direct current (DC) and radio frequency (RF) magnetron sputtering produce films with a limited range of properties available for tuning [29,39–43]. A significantly wider range of the properties with no need for post-deposition annealing can be offered by high power impulse magnetron sputtering discharges (HiPIMS), where a high fraction of ionized and field accelerated energetic species impinging the surface of the film [43–47].

In this work, we report a comprehensive study on the properties of ITO films responsible for their effective application in both optical and electrochemical sensing systems. We have analyzed the effect of reactive gas composition during HiPIMS discharges on tailoring crystallography of the ITO film, which subsequently determines the LMR conditions, as well as the electrochemical response. We have focused on the identification of deposition conditions, at which both electrochemical and optical interrogations are effectively and simultaneously possible. Finally, for the LMR optical fiber probe with tailored ITO coating, we discuss antibody detection in both electrochemical and optical domains.

2. Experimental details

2.1. Deposition setup

Reactive HiPIMS deposition of ITO thin film was carried out in a high-vacuum chamber capable for reaching the back-down pressure of 10^{-5} Pa and assure the high purity of the deposition. A commercial planar 3-inch in diameter magnetron was installed in configurations depending on the type of the applied substrates as shown in Fig. 1, i.e., in the upper part of the vacuum chamber or its sidewall. The magnetron was equipped with a compound ITO target (In_2O_3/SnO_2 of composition 90/10 wt% and a purity of 99.99 %). The sputtering was driven using pulsed power supply described elsewhere [48] with repetition frequency 1.5 kHz, duty cycle 10 %, and pulse width 66.7 μs. The experiments were carried out at constant mean power $P_m = 150$ W. The pressure was kept constant for all the experiments at $p = 0.5$ Pa. Inert argon (flow $f_{Ar} =$ 100 sccm), reactive oxygen and nitrogen (flow f_{O_2} and f_{N_2} varied in the range 0–55 sccm), all with a purity of 99.999 %, were used. The reactive gas concentration in the gas mixture c_R was estimated as $c_R = \frac{f_R}{f_{Ar}+f_R}$, where R denotes concentrations of O_2 or N_2.

The ITO films were deposited on Si(100) and glass substrates, both placed 15 cm away from the sputtering target. These flat substrates were used to analyze such ITO film properties as crystallography, electrical resistivity, optical properties (n and k), electrochemical performance, thickness etc. Furthermore, for LMR measurements, the optical fiber samples were coated too in the same deposition conditions except the magnetron installation (Fig. 1). We used approx. 15 cm long multimode polymer-clad silica fibers with 400/730 μm (core/cladding) diameter, where out of a central part (25 mm) of the fiber the cladding was removed and after ITO deposition it served as an active sensing area. The fiber was rotated during the deposition to receive a uniform ITO coating around it.

2.2. Analytical methods

The surface morphology of flat reference substrates was investigated using atomic force microscopy (AFM Pico SPM, Agilent Technologies) operating in tapping mode. Film crystal phase analyses were performed by grazing incidence X-ray diffractometry (XRD) described elsewhere [49]. We used a D8 ADVANCE diffractometer (Bruker AXS) with Cu Kα radiation (40 kV, 40 mA). The quantitative phase analyses were based on Rietveld calculations (Topas 5, Bruker). Scanned 2θ range was from 15° to 80° at an incidence angle $\omega = 1°$. The resistivity of ITO samples was measured by a four-point probe supported by a Keithley 2400 current source meter, where needle-like probes with 100 μm radius were placed in a straight line with equal inter-probe spacing ($s = 1.5$ mm). Due to the finite sample size (10 × 25 mm), a correction factor 0.867 was taken into account for resistivity (ρ) estimation [50].

Optical properties of the deposited ITO film were investigated using Woollam M-2000XI variable angle spectroscopic ellipsometer working in range $\lambda = 210 - 1690$ nm and angles of incidence 55°, 65°, and 75°. Measurement data were fitted to a layer model of the investigated structure, where ITO with a roughness layer was placed on the Si substrate. Dielectric function of the ITO film was modeled by the Tauc-Lorentz oscillator. In the case of samples with added oxygen, the Tauc-Lorentz oscillator was supplemented by the Gaussian oscillator. Thicknesses of the films were almost the same for all the samples. Thickness-independent attenuation coefficient μ was estimated according to relation $\mu = 4\pi k/\lambda$, where k and λ are extinction coefficient of the film measured by the ellipsometry and corresponding wavelength, respectively [51]. The transmittance T of the films for $\lambda = 200 - 1100$ nm was investigated using a double-beam UV–vis spectrophotometer (Shimadzu UV-1800).

The electrochemical performance of the films was tested in cyclic voltammetry (CV) configuration using an Autolab, Metrohm Autolab

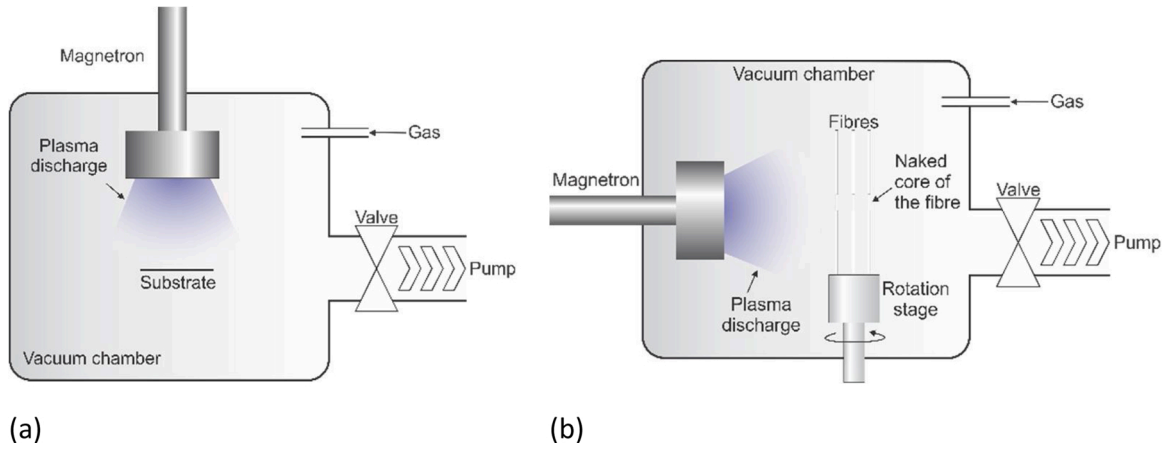

Fig. 1. The experimental setup used for deposition on (a) flat substrates and (b) on optical fibers.

PGSTAT128 N potentiostat/galvanostat controlled by GPES software. The ITO films deposited together with Si also on glass slides (8 mm diameter) were used as working electrodes (WE), where a platinum wire and an Ag/AgCl 0.1 M KCl were used as a counter electrode (CE) and a reference electrode (REF), respectively. All the measurements were performed at room temperature in a solution of 0.1 M KCl (POCh, Poland) containing 1 mM 1,1′-Ferrocenedimethanol (Acros Organics) as a redox system. All cyclic voltammograms were obtained in the potential range from -0.25 to 0.6 V vs. Ag/AgCl electrode at a scan rate of 100 mV/s.

The optical transmission of the ITO-LMR structure on an optical fiber was interrogated in the range $\lambda = 350 - 1050$ nm using Ocean Optics HL-2000 white light source and Ocean Optics USB4000 spectrometer [29]. The spectra were obtained by subtracting the reference spectrum of the used light source T_0 from the optical transmission spectrum T_{LMR} of the sample. The sensitivity of the samples to changes of external RI (n_{ext}) was determined by immersing the sample in water/glycerin solutions of different concentrations ($n_D = 1.357 - 1.404$ RIU). Reichert AR200 refractometer was used to verify n_{ext} of the solutions.

To identify both electrochemical and optical performance for label-free sensing, the LMR sensor with ITO film surface has been bio-functionalized towards the specific binding of an analyte. First, the ITO-LMR sensor was consecutively cleaned in isopropanol and water and dried under a stream of argon. Next, surface silanization with 3-triethoxysilylpropyl succinic anhydride (TESPSA) was performed according to the procedure described by *Gang et al.* [52] The reaction was carried out for 4 h. Primary and secondary antibodies targeted *Borrelia burgdorferi* have been used as receptor and target, respectively. The succinic anhydride reacts with amines in the ring-opening reaction to form amide bonds. In the next step, the sensor was incubated for 30 min in a solution of the primary antibodies (10 μg/mL) to covalently bond them to the surface. This step was followed by extensive washing with PBS. The concentration of the receptor at the ITO-LMR surface was determined by means of the procedure described elsewhere [53]. The incubation buffer concentration of antibodies (Borrelia burgdorferi receptors) was 10 ug/mL, therefore $\sim 4 \times 10^{13}$ of antibodies were available for the functionalization process. As the area of the cylindrical LMR sensor is ~25 mm^2, and the area of an antibody is ca. 10 nm^2, we assume that the optical fiber's surface is covered with up to 2.5×10^{12} interaction units. Next, the sensor surface was immersed in a BSA solution (0.5 mg/mL in PBS) for 30 min to block any remaining unspecific sites. The washing procedure was repeated as described earlier. For the sensitivity analysis, the sensor was immersed in increasing concentrations (1, 5, and 10 μg/mL) of the secondary antibody for 30 min in each solution. Incubation in every concentration was followed by extensive washing with PBS. During each incubation step, the optical signal of the LMR sensor was monitored in the range of $\lambda = 350$–1040 nm every 1 min. At each step of the experiment after the incubation and washing the samples have been placed consecutively in PBS and 1 mM Ferrocenedimethanol (in PBS) and underwent CV at scan rate of 20 mV/s for 3 cycles in the potential ranging from -0.5 to 1.5 V with simultaneous optical monitoring.

3. Results and discussion

Our previous works [29,43] indicated contradictory deposition parameters for obtaining ITO films suitable for LMR and those showing electrochemical activity. To broaden the range of properties, we investigate here the effect of oxygen and/or nitrogen doping as the agents for tailoring the ITO properties.

3.1. Crystalline structure of ITO

The presence of reactive gases strongly influences phase formation of deposited ITO films. In the case of pure *Ar* discharge, i.e., without any reactive admixture, the XRD reveals two crystalline phases - 92.2 wt% ITO and 7.8 wt% metallic indium (Fig. 2(a)). The lattice parameter of ITO in these conditions is $a_{ITO} = 1.01655$ nm, while metal indium crystalizes with lattices $a_{In} = 0.32510$ nm and $c_{In} = 0.49502$ nm. Sub-stoichiometric, i.e., not sufficiently oxidized ITO films were reported in other works when employing RF sputtering. *Terzini et al.* [54] have shown that an increase of RF power density promotes oxygen vacancies and deposition of metal-like ITO films. This was observed for power densities exceeding 0.75 W/cm^2. In our case, the peak power density reaches over 60 W/cm^2. Hence, the formation of metallic *In* fraction in pure *Ar* discharge is not surprising. It is worth mentioning that in work by *Senol* et al. the preference of (222) crystal plane orientation was attributed to the presence of the oxygen vacancies that resulted in lower resistivity of the films [55].

When reactive O_2 was added, despite the peak power increase (by up to 25 % for $c_{O_2} = 10\%$), the vacancies were occupied and resulted in crystalline ITO deposition (Fig. 2(b)). Slight doping of the discharge by oxygen ($c_{O_2} = 0.5\%$) is sufficient for formation of crystalline ITO with no XRD peak related to metallic *In* observed, and even more increased lattice parameter $a_{ITO} = 1.0184$ nm. For further increase of c_{O_2}, the formation of crystalline ITO structure is significantly disturbed. For these films, smaller lattice sizes were found indicating their over-stoichiometry (Fig. 3). Such an effect indicates that sputtering in pure *Ar* atmosphere results in sub-stoichiometric films and some oxygen needs to be incorporated to attain pure crystalline ITO films. This effect becomes pronounced specifically for HiPIMS discharges, where the target is loaded by high peak power, and sputtered species are not fully saturated by oxygen.

Change of crystallization was observed also, when N_2 was employed

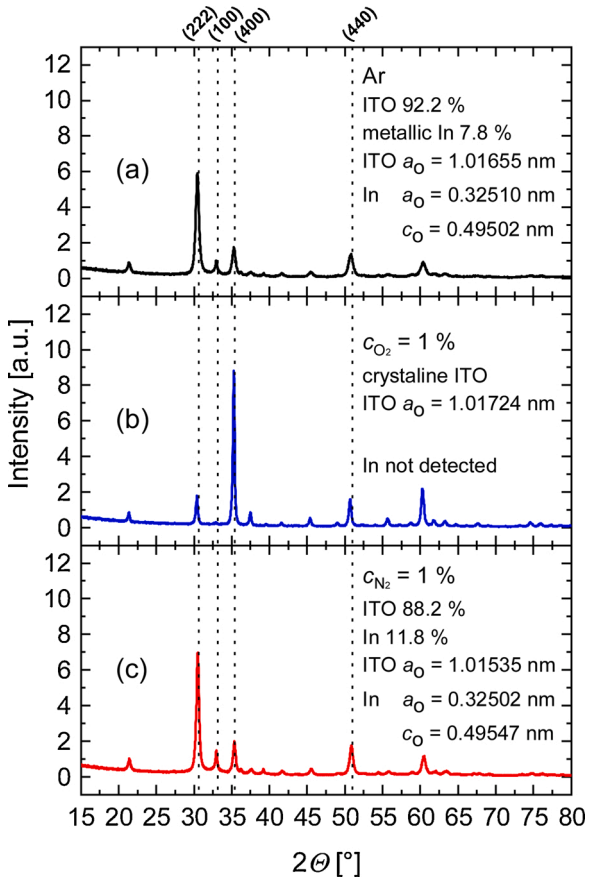

Fig. 2. Selected XRD patterns of ITO films deposited at different concentrations of the reactive gas, (a) corresponds to pure *Ar*, (b) c_{O_2} = 1%, and (c) c_{N_2} = 1%. The deposited film has to be slightly doped with oxygen to form crystalline ITO. Without oxygen doping, a fraction of metallic *In* appears in the films what is indicated by peak (100).

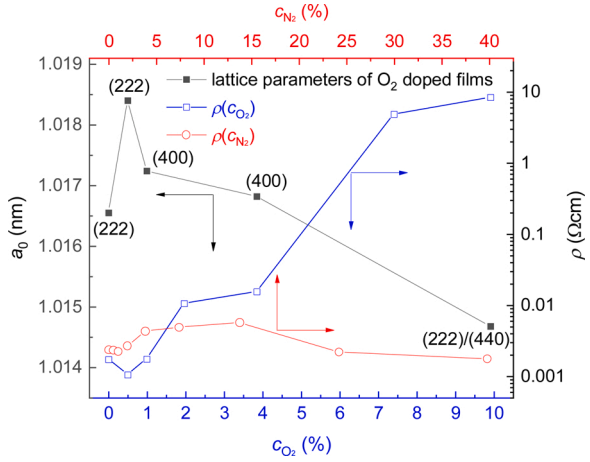

Fig. 3. Evolution of lattice parameter a_0 (left axis) and resistivity $\rho_{N2,\ O2}$ (right axis) with concentrations of reactive process gases c_{O_2} and c_{N_2}. Different scales for horizontal x-axis related to c_{O_2} (the lower x-axis) and c_{N_2} (the upper x-axis) has been applied. The lattice parameters for films prepared in *N_2/Ar* are not shown due to their amorphous nature.

as a reactive gas. In this case, we observed a higher intensity of the dominant (222) peak that was attributed to the sub-stoichiometric character of ITO (Fig. 2(c)). An effect of the increased peak was observed also in our earlier work [43], where it was corresponding to energy stored in vibrational and rotational states of nitrogen molecules. This energy is delivered to the growing film and it affects the crystallization process. The same mechanism was indicated to be responsible for the improved growth of TiO_2 films [56] and it is expected to be responsible for the growth of ITO films with metallic *In* too. It is important to note that ITO crystallization is improved only up to a certain level of *N_2* doping, i.e., for $c_{N_2} < 4\%$ the film is polycrystalline with dominant (222) peak and the further increase of nitrogen flow promotes amorphous film. Films deposited at $c_{N_2} = 1\%$ reveal again a phase mixture of ITO and metallic *In*. The mass fraction of metallic *In* is 11.8 % and it is higher than in films deposited in a pure *Ar* atmosphere. The *In* lattice parameter are $a_0 = 0.32502$ nm and $c_o = 0.49547$ nm. The lattice parameter, the same as properties of the films deposited in the pure *Ar,* are practically identical as for pure *In* ($a_0 = 0.0.3252$ nm and $c_o = 0.49466$ nm) [57]. However, higher nitrogen flows prevent not only from the formation of the crystalline ITO, but also crystalline metallic *In*. The patterns for films deposited at $c_{N_2} > 4\%$ indicate their amorphous state. Nevertheless, the detection limit of the employed method is about 3 nm particle size, what makes it difficult to clearly confirm the fully amorphous structure of the films and impact of metallic *In* on their physical properties.

As it is shown in Fig. 3, for all the deposited ITO films phases show lattice parameter higher than for pure In_2O_3 ($a_0 = 1.0117$ nm) [58] and $In_{0.9}Sn_{0.1}O_{3.02}$ ($a_0 = 1.0124$ nm and $a_0 = 1.0126$ nm reported by *Quaas* et al. [58] and by *Gonzales* et al. [59], respectively). When compared to metallic *In*, all the investigated ITO films show a defect structure. Changes in the structure of ITO films could be caused by non-equilibrium HiPIMS deposition conditions. The repulsion forces arising from the extra positive charge of the *Sn* cations cannot explain changes in the lattice parameters [59]. We propose an explanation based on the impact of (i) large compressive stress produced by atoms irregularly built in the hosting structure and (ii) a mechanical interaction between regions (nanocrystals) with different lattice parameters.

Moreover, the $a_0(c_{O_2})$ shown in Fig. 3 indicates the preferred orientation (the most intensive XRD patterns) in the film. We can observe the evolution of the preferential planes, i.e., (222) for $c_{O_2} < 0.5\%$, (400) for $1.0\% < c_{O_2} < 7\%$ and again dominant (222) peak, but highly competing with (440) as the c_{O_2} ratio further increases.

The fact that ITO crystalizes in different preferred orientations has not been fully understood yet. However, since the other deposition factors, i.e., substrate temperature, pressure, distance from the magnetron, etc., were kept constant, the observed behavior is attributed to plasma parameters and plasma-substrate interaction. *Zhao et al.* [60] have shown that (222) orientation is deposited at lower power density while the (400) peak becomes dominant for films deposited at higher power. It could be caused by (*i*) re-sputtering of the deposited ITO film by impinging energetic species and (*ii*) mobility of the adatoms on the surface since mobility is strongly influenced by energy delivered to the substrate. At the very beginning of the film formation, nucleation centers with different orientations grow on the substrate surface. Although the (400) orientation is reported as the most resistant against re-sputtering [54] and is more thermodynamically favorable [61] when compared to (222) orientation. Adatoms need to have higher mobility, i.e., energy, to form (400)-oriented nucleus. The (222) orientation of the grains is reported to be dominant at the initial stage of the growth for any deposition conditions. This might be attributed to *In* metal adatoms aggregating into (111) planes of face-centered tetragonal structure which are very close to (222) planes of ITO bixbite structure [61]. Experiments with low or zero oxygen concentration exhibited lower peak power density, which might reduce the mobility of the adatoms on the surface needed for (400)-oriented growth. However, due to lower incoming energy, the re-sputtering process of (222)-oriented nuclei was limited too. On the contrary, their development was stimulated by the presence of metallic *In* structures mentioned above. The peak power rises with increasing oxygen concentration what causes: (i) re-sputtering of (222)-oriented grains together with (ii) increased mobility of the

adatoms enabling their attachment with thermodynamically favorable (400)-nuclei [60].

Nevertheless, over-saturated oxygen gas mixtures in the deposition process can enhance the oxidation of the metal species impinging the substrate with reduced surface mobility. These deposition conditions were done with increased peak sputtering power - reduced accelerating voltage decreases average kinetic energy of incoming particles, what suppresses the re-sputtering of (222)-oriented crystallization centers and their preferential growth. It can be also expected that a smaller fraction of the delivered oxygen was transformed into reactive form and therefore vibrational states of the remaining O_2 molecules can contribute significantly to the transfer of heat to the substrate. This assumption is supported by observed both (222) and (440) plane reflections that are typical for annealed ITO films [55]. In this regime, the O_2 molecules may have a similar role as N_2 molecules in the experiments where a small amount of nitrogen was added to the discharge. Finally, the experiments prove that HiPIMS deposition provides a possibility to achieve well-crystalline ITO films without the need for any annealing.

3.2. Electrical and optical properties of ITO films

As shown in Fig. 3, ρ of *O2/Ar* prepared films strongly depends on oxygen partial pressure and the profile of the lattice constant. The lowest resistivity ($\rho_{O2} = 10^{-3}$ Ω·cm) was measured for the largest lattices and domains. It is well known that films with large domains exhibit improved conductivity because electron mobility is limited by scattering at the grain boundaries and ionized impurities (*Sn*-ions in ITO) [62], while increasing oxygen concentration increases ρ due to the formation of stable *Sn-O* complexes [63]. The same effect was observed for films prepared in the *N2/Ar* atmosphere. The lowest ρ was achieved for films deposited in a slightly oxygen-containing atmosphere ($c_{O_2} = 0.5\%$). However, while ρ is rather gas-composition-independent for low concentrations ($c_{O_2,N_2} < 1\%$), it becomes dependent on the composition for higher concentrations of reactive gases. While ρ_{N2} is more or less constant with the concentration, ρ_{O2} rises by several orders of magnitude. Lower ITO resistivity of samples prepared at higher nitrogen concentration could be caused by nitrogen creating acceptor levels above the valence band, which increases the concentration of carriers and subsequently also reduces. Low ρ of films deposited in the pure *Ar* atmosphere, nitrogen admixtures, and low oxygen admixtures (for $c_{O_2} < 1\%$) can be also influenced by the content of metallic *In*. It is worth to remind that ρ was measured on as-deposited samples without any post-processing.

For optical sensing purposes of ITO, its optical properties play a crucial role. Hence, *n*, attenuation coefficient (μ), and transmittance (*T*) were studied for different c_{O_2} and c_{N_2}. It is well known, that the ITO absorbs UV radiation for $\lambda < 350$ nm and it is confirmed by our experiment. The effect corresponds to a fact that ITO is a heavily-doped n-type semiconductor with a rather large bandgap of about 4.5 eV [64,65]. Based on ellipsometric data we investigated $\mu(\lambda)$ calculated as $\mu = 4\pi k/\lambda$. The μ at λ = 530 nm for different gas concentrations was shown in Fig. 4. It must be noted that different scales were applied in the x-axis for c_{O_2} and c_{N_2}. The wavelength was selected specifically for cross-correlation purposes, as it is positioned far enough from the ITO absorption edge and represents the film properties in visible spectral range, where a variety of optical sensors operate. A similar relation between the optical properties of ITO could be observed across the entire useful for optical sensing applications spectral range with minor changes in magnitude. The highest μ values were measured for $c_{N_2} = 2\%$, when ITO is well-crystallized. Generally, the highest decrease in μ was achieved by slight oxygen doping of the process gas ($c_{O_2} = 2\%$). We attribute this effect to more effective crystallization at these conditions. From the point of view of optical properties, sub-stoichiometric films deposited in pure *Ar* discharge can be significantly improved by slight oxygen doping. In general, a higher concentration of oxygen or nitrogen further improves μ. This finding also corresponds to ρ measurement. The

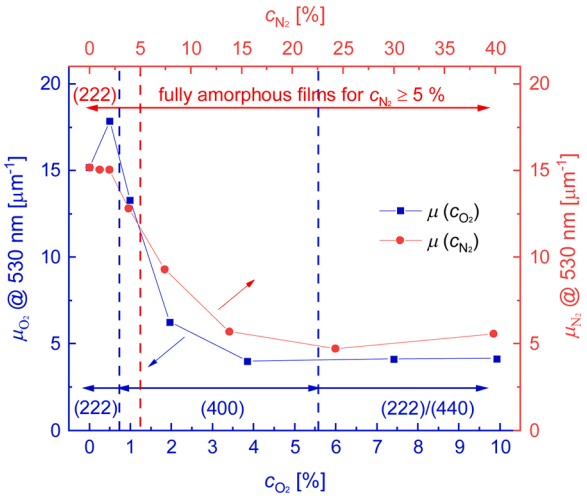

Fig. 4. The dependence of the attenuation coefficient μ on reactive gas concentrations c_{O_2} and c_{N_2}. Different scales for horizontal x-axis related to c_{O_2} (the lower x-axis) and c_{N_2} (the upper x-axis) were applied for comparison. The brackets denote dominant crystal orientation.

reason behind the absorption drop in the case of the nitrogen addition could be caused by a reduced release of oxygen species from the sputtered material.

3.3. Tailoring ITO film properties for electrochemical sensing

The electrochemical response of ITO films deposited on glass slides is discussed in this section. In all the electrochemical measurements, 1,1′-Ferrocenedimethanol was used as an outer-sphere redox system due to the solubility in aqua solution and lack of its adsorption to the electrode during the electrochemical process [66,67]. Additionally, these redox species undergoes fast reactions at the ITO electrode [68].

The CVs for selected ITO films prepared at c_{O_2} up to 10 % and used as a working electrode are shown in Fig. 5. The redox reactions of 1,1′-Ferrocenedimethanol are observed in all the measurements as two well-defined current peaks. The shapes of the CVs prove that all the electrodes exhibited high reversibility of the redox reaction. The potential separation between anodic (I_{pa}) and cathodic peak current (I_{pc}) noted as ΔE for the ITO electrode prepared at $c_{O_2} = 0\%$ is equal to 149 mV and the current ratio (I_{pa}/I_{pc}) is near to 1. These results suggest a single electron quasi-reversible electrochemical redox process [69]. It is worth noting

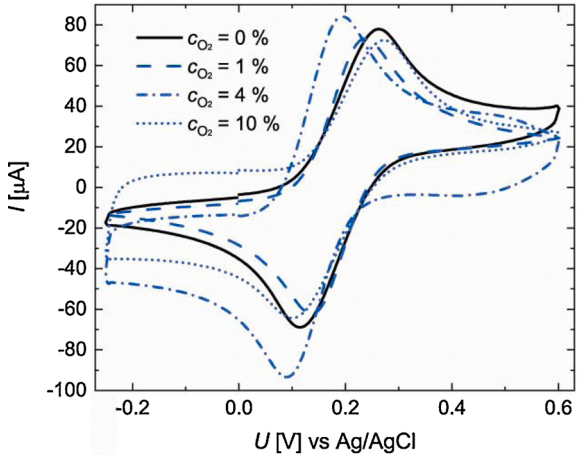

Fig. 5. Cyclic voltammograms at scan rate 100 mV/s for measurements in 1 mM 1,1′-Ferrocenedimethanol in 0.1 M KCl for ITO-coated glass slides received at different gas concentrations.

that the ΔE initially slightly decreases and further increases with c_{O_2}, i. e., ΔE is equal to 119 mV, 103 mV, and 173 mV for $c_{O_2} = 1\%$, 4%, and 10 %, respectively. This phenomenon indicates that electron transfer is disturbed less for the films obtained at c_{O_2} reaching 1–4%. Subsequently, for the samples prepared in the O_2 enriched atmosphere $c_{O_2} > 4\%$, the noticeable changes are observed in the shapes of the obtained voltammograms for the negative potential, what is probably associated with increased capacity of the electrode and its worse electrochemical sensing performance.

The effect of the reactive gas doping, i.e., c_{O_2} and c_{N_2}, on the electrochemical response has been compared in Fig. 6. A similar trend as for c_{O_2} has also been observed in the case of nitrogen doping. For small c_{N_2} a slight improvement of ΔE occurs, most probably due to improved crystallinity, was observed that was followed by an increase of $\Delta E \approx$ 600 mV for $c_{N_2} > 5\%$ when the ITO structure becomes amorphous. The obtained data indicate a strong correlation of the ΔE and the crystallinity, i.e., films with well-pronounced crystallinity reach $\Delta E \approx 100 -$ 200 mV for both the gases, what is comparable or lower than values obtained for ITO electrodes prepared at similar conditions, but using RF sputtering instead of HiPIMS [29]. In the case of the oxygen doping, a slight increase of ΔE apparently follows the trend for ρ (Fig. 3). However, ρ shows a minor impact, when compared with the effect of the crystallinity. Hence, the results revealed that rather the crystallography than ρ determines $\Delta E(c_{O_2}, c_{N_2})$. Since for electrochemical sensing applications, ΔE should be as low as possible, the selection of low concentration of the doping gases (up to 4%) is preferred.

3.4. Tailoring ITO film properties towards applications in optical sensing

In this section, we discuss the impact of optical properties of the films on the optical response of an optical sensor using a LMR optical fiber device. For receiving LMR and its sensing applications both optical properties of the film, as well as its thickness, are crucial. Thus, the selected sensing platform can be treated as suitable for discussing general optical sensing applications of the ITO films, especially where those for RI or biosensing are concerned. In the previous section, the ITO film characterization was carried out on planar Si or glass samples where the films for comparison purposes had nearly the same thickness regardless on the deposition conditions. The LMR response was measured for optical fiber devices coated exactly in the same deposition conditions as planar samples, but with a different thickness that is required for receiving LMR response in a specific spectral range. Fiber rotational assembly, as shown in Fig. 1(b), allowed for depositing homogeneous ITO films on a fused silica fiber core. Since the deposition conditions were kept the same, we assume here similar properties of the films on a planar substrate and the fiber surface.

The thickness of the films on each fiber was optimized to observe a well-pronounced LMR in the wavelength range between 550 and 600 nm when the sensor was surrounded by air. We are aware that the sensors would be more sensitive when the resonance was positioned at longer wavelengths. The reason behind the resonance positioning in this range was to keep the response in the operation range of the applied spectrometer and light source for the whole range of the n_{ext}. Moreover, to maintain the high sensitivity of the sensor, the lower order of LMR should be traced, and those appear for lower thicknesses of the overlays [5]. For this reason, we continued the deposition only up to the point when the LMR was well pronounced. The RI sensitivity was estimated as $S = \delta\lambda_{LMR}/\delta n_{ext}$, where λ_{LMR} denotes as resonance wavelength corresponding to a minimum in the T (Fig. 7). The method of measurement has been described elsewhere [70,34]. For the purpose of this work, the sensitivity was determined in the n_{ext} range of 1.357–1.404 RIU.

In Fig. 7 is shown the shift of LMR response with n_{ext} for the fiber coated with ITO at $c_{O_2} = 4\%$. It is worth noting that for sensors prepared in pure *Ar* or *N2/Ar* with low c_{N_2} no LMR effect was observed and for those sensors prepared at high c_{N_2} relatively low sensitivity (193–314 nm/RIU for $c_{N_2} = 4\%$ and $c_{N_2} = 24\%$, respectively) was reached when compared to those achieved for ITO deposited at higher c_{O_2}. Such sensitivity is comparable to that measured for RF sputtered ITO [70]. That is why in this discussion we will focus more on oxygen- than nitrogen-doped films. The inset in Fig. 7 shows the RI sensitivity of the ITO-LMR sensor received for different c_{O_2}. The sensitivity increases with the concentration of oxygen in the discharge up to 513 nm/RIU (for $c_{O_2} = 10\%$), which is noticeably higher than in the case of applied conventional RF sputtering [70], where the films are typically amorphous if not annealed [41].

In Fig. 8(a) can be seen that the resonance depth is the highest for discharges with a low amount of oxygen, and becomes lower with increasing oxygen concentration in the discharge. Hence, the LMR depth is inversely proportional to the oxygen concentration. The depth can be mostly correlated with k of the film. Fig. 8(b) presents the dispersion relation for n and k measured on flat substrates corresponding by their deposition conditions to the sensors presented in Fig. 8(a). The comparison indicates that higher oxygen flows induce a reduction in k (comparable to relation for μ in Fig. 4) what makes the resonance shallower [5]. In other words, for the formation of deep LMR only slightly absorbing film with a high n are expected. A different character of the LMRs in the case of samples prepared at $c_{O_2} > 0.5\%$ is caused also by different n and k. Both the optical parameters tend to decrease with

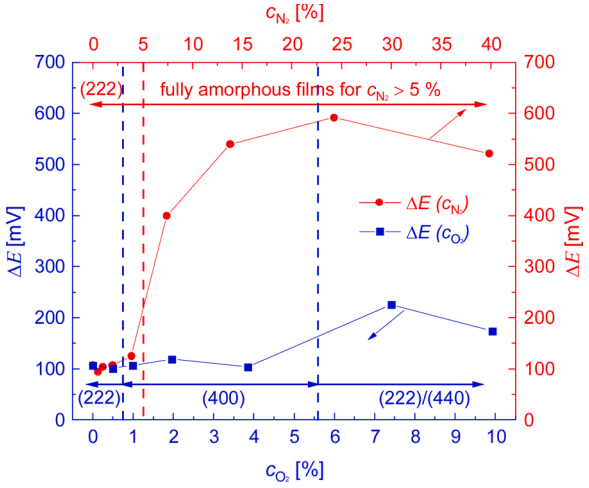

Fig. 6. Evolution of the current peak separation with the concentration of the reactive gases $\Delta E(c_{O_2}, c_{N_2})$. Different scales for horizontal x-axis related to c_{O_2} (the lower x-axis) and c_{N_2} (the upper x-axis) were applied for comparison. The brackets denote crystalline orientation.

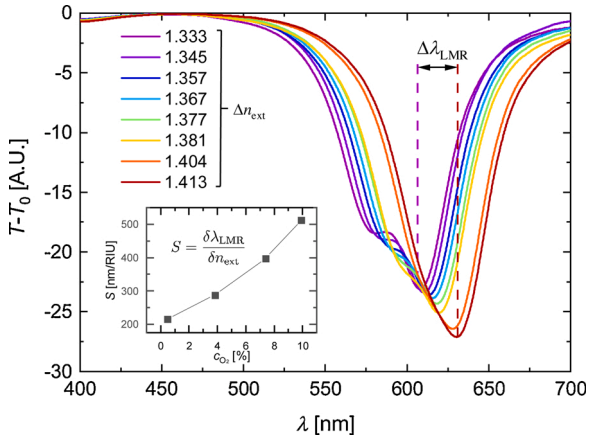

Fig. 7. Evolution of LMR response caused by a change of the external RI for the ITO-LMR sensor prepared at $c_{O_2} = 4\%$. Inset shows RI sensitivity for sensors received at different c_{O_2}.

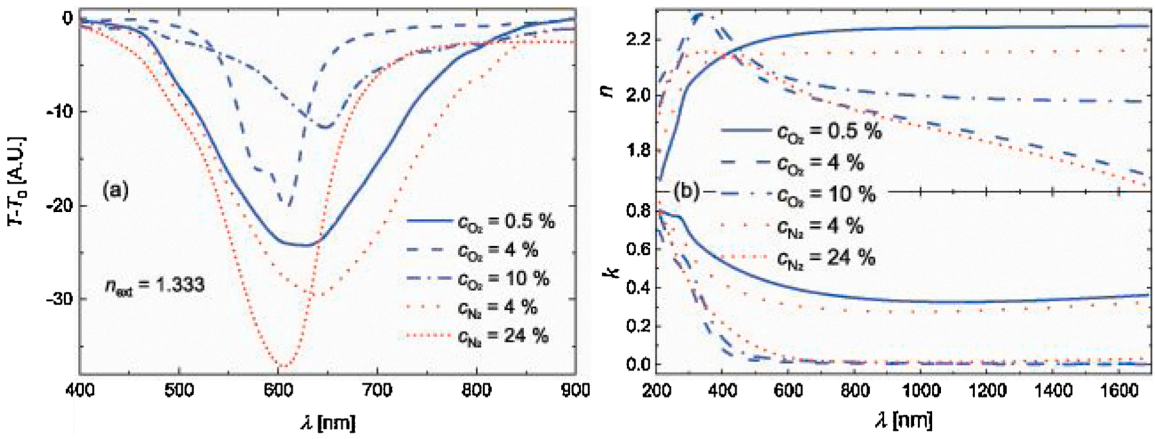

Fig. 8. (a) LMR spectrum for optical fiber sensors coated at different gas composition when immersed in water, and (b) corresponding refractive indices and extinction coefficients of the ITO films deposited at the same conditions on flat substrates.

c_{O_2}, while the RI sensitivity increases from 216 nm/RIU to 513 nm/RIU for $c_{O_2} = 0.5$ % to $c_{O_2} = 10$ %, respectively (see inset in Fig. 7). To identify the reasons for the increase in the sensitivity, profilometry and in situ quartz crystal microbalance measurements were used to estimate the deposition rates. These were roughly the same regardless on the oxygen concentration in the discharge. However, due to a decrease in n with c_{O_2}, to obtain the well-visible LMR the deposition time had to be gradually increased, so that it was almost two times longer for deposition at $c_{O_2} = 10\%$ than at $c_{O_2} = 0.5\%$. Therefore, we attribute the increasing RI sensitivity of the sensors prepared in the oxygen-enriched atmosphere to the increasing thickness of the ITO films [5]. It must be noted that the nitrogen-enriched mixtures result in very well-pronounced LMR too, but for the concentration significantly higher than for doping with oxygen (Fig. 8). However, their sensitivity is rather low (193 nm/RIU for $c_{N_2} = 4\%$) comparing to those shown in Fig. 7, where the one for c_{O_2} is concerned. The fact that for samples prepared without oxygen or with a low concentration of nitrogen no LMR is observed suggests that the obtained samples with higher k are close to the edge of the properties acceptable for LMR at these experimental conditions (Fig. 4) [71]. For this reason, even a small change of deposition parameters can influence the LMR properties dramatically.

3.5. ITO for optical and electrochemical label-free biosensing

Detection of the pathogen (Borrelia burgdorferi) was carried out to demonstrate the advantages of detailed material research of electrochemically-active LMR sensor surfaces. Simultaneous, dual-domain optical and electrochemical measurements were conducted in the same analytes to prove the concept of cross-verification in the detection procedure. For this part of the experiment, we prepared a batch of ITO-LMR sensors with ITO properties tailored by plasma procedure to obtain well-pronounced electrochemical activity and optical response corresponding the results received at $c_{O_2} = 4\%$.

When it comes to detection of, e.g., pathogens, it is possible inter alia, indirectly through the presence of antibodies synthesized in a body during an infection. In this case, sandwich immunoassays are one of the most frequently applied. Two antibodies (primary and secondary) synthesized against *Borrelia burgdorferi* have been utilized as a receptor and specific target, respectively. Primary antibodies were covalently immobilized to the ITO-LMR surface (see Section 2.2) through the silanization process. Next, they were captured/recognized by secondary antibodies in the following step of the experiments. These, in turn, allowed to verify the ability of the ITO-LMR for label-free sensing and to estimate the sensitivity of the platform. Thanks to the optimized ITO properties, during the experiment both EC and optical measurements were performed.

First, it must be noted that the ITO-LMR sensors investigated here reveal slightly different EC performance versus that achieved for flat reference samples shown in Fig. 5. Only investigated in Section 3.3 flat substrates allowed for correlating EC and optical properties of ITO, where later were measured using spectroscopic ellipsometry, which is not suitable for analysis of the thin film properties on other than flat substrates. Possible differences between properties of ITO films deposited on the flat and circular substrate at the same deposition conditions have already been reported in [29] for ITO electrodes deposited using RF sputtering. The differences were attributed to the sample shape disturbing discharge resulting in a partially non-stoichiometric composition of deposited films [72]. For such ITO, charge transfer caused by local charge blocking barriers is less effective [73]. However, the difference between the EC performance is not crucial for the ITO biofunctionalization and the final detection of pathogens. For the fiber sample a decrease of anodic and cathodic peak currents that indicate successful silanization of the surface but also a partial limitation of its electrochemical activity (Fig. 9(a)). It must be noted that the applied surface modification offers important advantages – it is an easy, one-step reaction, thus does not need any additional activation. However, the shortage of the reaction time (4 h), thus, control over the thickness of the silane layer, is always at the expense of its quality and stability. Therefore, it is recommended to carry out the reaction for 4 h [52].

Fig. 9(b) shows, in turn, the evolution of the optical spectra at each step of the experiment. The shift towards longer wavelengths (indicated by the black arrow) corresponds to an increase of the thickness of the biological layer on the functionalized ITO-LMR's surface, additionally confirming the electrochemical results. Next, both optical and EC responses followed the antibody-antibody interaction. When target antibody concentration increases, a decrease in current and increase in LMR wavelength shift were recorded in the EC and optical domain, respectively, proving binding of the antibodies to the sensor's surface. It can be also noted that measurements in the EC domain are effective when interactions at the sensor surface take place, while optical measurements may deliver information about events taking place slightly away from the surface. Notwithstanding, the changes after further steps of the experiment, such as increasing ΔE, are still clear and indicate binding of the receptor and different concentrations of the target. It is worth to mention that the difference between the initial ΔE described in the paper and here is a result of lower scan rate (20 vs. 100 mV/s). The rate has to be reduced due to time required for simultaneous acquisition of the optical data.

Fig. 10(a) presents the evolution of λ_{LMR} during the whole experiment. Oscillations observed in PBS and 1,1′-Ferrocenedimethanol at the stages corresponding to CV measurements are low in magnitude when compared to reported previously in [34]. The limited influence of the

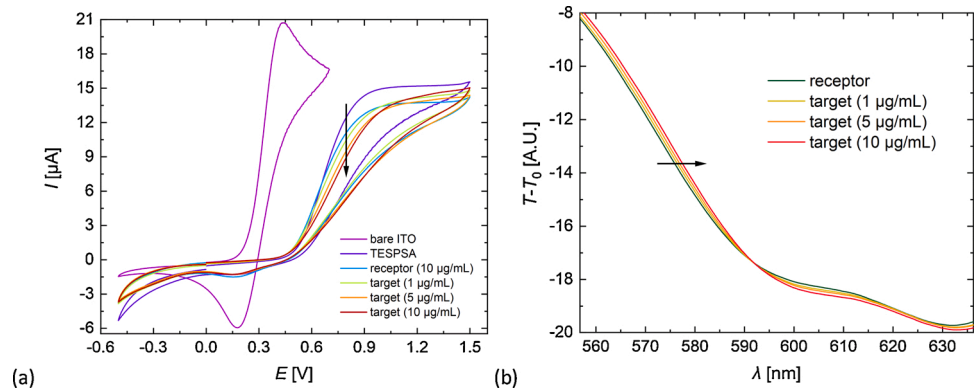

Fig. 9. EC and optical responses of ITO-LMR sensors recorded after each incubation step during process of Borrelia burgdorferi receptor-target interactions, (a) shows CV recorded at scan rate 20 mV/s in 1,1′-Ferrocenedimethanol and (b) optical spectra acquired in PBS.

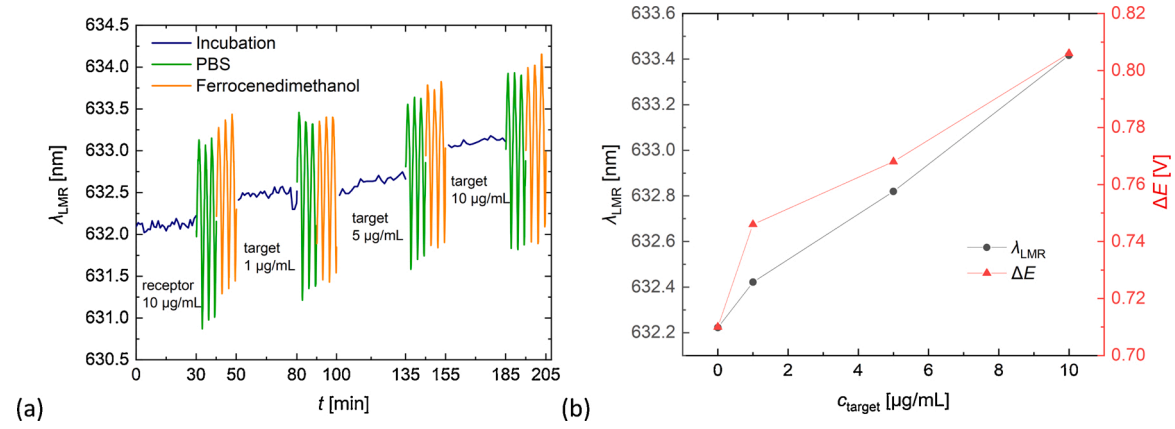

Fig. 10. (a) Sensogram for the ITO-LMR biosensing experiment and (b) comparison of ITO-LMR wavelength and ΔE shift at each step of Borrelia burgdorferi receptor-target interaction experiment. Oscillations seen in (a) correspond to the cycling potential.

applied *E* corresponds to higher doping of ITO investigated in this work. When the material is highly doped, a shallow charge accumulation layer is formed, and the modulation of the RI of ITO is low comparing to materials with low carriers concentration [29]. Moreover, a clear shift of the LMR wavelength towards longer wavelengths at the incubation stages and for an increase in target concentration can be seen. It can be seen in Fig. 10(b) that the trend for both electrochemical and optical measurements is very similar, thus we cross-verify the biosensing experiments. This is evidence that the tuning of the properties makes the verification possible.

In general, dual-domain sensing designs allow to increase the reliability of the measurements or/and extend the measurement range, as revealed in other works reporting protein detection achieved by means of electrochemical surface plasmon resonance [74], electrochemical optical waveguide [75], or electrophotonic silicon biosensing [76]. None of these dual-domain sensors have used the same receptor-target scheme, which is an immunoassay sandwich for antibody-antibody interactions detection. Thus, the direct comparison of these detection approaches is limited. Moreover, it must be emphasized that both high-performance EC[29] along with LMR [34] responses have not been achieved for non-optimized/un-doped ITO-based structures. Presented here results prove that crucial role of tailoring ITO properties for simultaneous optical and EC biosensing.

4. Conclusion

In this work, we have shown a comprehensive study on ITO film properties crucial for their application in combined optical and electrochemical sensing systems. For ITO deposition, we used high power pulse magnetron sputtering (HiPIMS) where high-quality films can be deposited in a single-step process. The applied approach does not require any post-processing, such as high-temperature annealing, which is typically needed when other deposition techniques are used. Application of other deposition methods requiring post-processing would possibly make it difficult to draw direct conclusions on the relation between deposition process parameters and properties of the films. Our experiments have shown that by tuning gas composition in the sputtering chamber it is possible to control the preferred crystal orientation of the films and both their electrical and optical properties. We have found that it is necessary to slightly enrich the deposition atmosphere by oxygen to reach fully oxidized and stoichiometric ITO. Moreover, on top of ITO resistivity, crystallinity mainly influences the electrochemical activity of ITO. We have observed that well-crystalline films exhibit excellent electrochemical properties. The optical properties of ITO are highly influenced by gas composition too. Low concentration of oxygen or nitrogen results in receiving films showing high refractive index and extinction coefficient in the visible and near-infrared spectral range. Both the parameters decrease with the concentration of the gases (investigated up to 10 % and 40 % for oxygen and nitrogen, respectively), where for the concentration of oxygen reaching 4% the extinction coefficient is low as it is expected by the majority of optical applications. Later, we have shown one of the applications - a lossy-mode resonance (LMR) obtained using the ITO-coated optical fibers. The most suitable LMR conditions were found for the relatively low extinction coefficient where the resonances are well-defined as expected for sensing applications of the device. The refractive index sensitivity, which is crucial for chemical and biochemical label-free sensing applications of the sensors, increases with the concentration of the two gases,

but the application of oxygen was found to be more effective than nitrogen.

To summarize, both electrochemical and optical interrogations of ITO-coated sensors can be simultaneously achieved when HiPIMS deposition is applied. Highly crystalline films are expected for electrochemical applications, and those can be obtained at low concentrations (below 5 %) of oxygen or nitrogen in the sputtering atmosphere. However, properties expected for optical applications get more attractive with an increase in the concentration of the gasses. For these conditions optical absorption of the films decreases, especially in the case of oxygen admixtures, when the structure becomes amorphous. Thus, as identified in this work there is a narrow range of ITO film properties, where the films can be simultaneously applied in a wide selection of combined label-free optical and electrochemical sensors, including biosensors with enhanced functionalities.

CRediT authorship contribution statement

P. Sezemsky: Investigation, Data curation, Visualization, Writing - original draft, Writing - review & editing. **D. Burnat:** Investigation, Data curation. **J. Kratochvil:** Investigation, Data curation. **H. Wulff:** Investigation, Data curation. **A. Kruth:** Investigation, Data curation. **K. Lechowicz:** Investigation, Data curation. **M. Janik:** Methodology, Writing - original draft, Writing - review & editing. **R. Bogdanowicz:** Formal analysis, Funding acquisition, Writing - review & editing. **M. Cada:** Investigation, Data curation. **Z. Hubicka:** Investigation, Data curation. **P. Niedziałkowski:** Methodology, Investigation, Data curation. **W. Białobrzeska:** Investigation, Data curation. **V. Stranak:** Funding acquisition, Project administration, Conceptualization, Methodology, Formal analysis, Supervision, Resources, Writing - original draft, Writing - review & editing. **M. Śmietana:** Funding acquisition, Project administration, Conceptualization, Methodology, Formal analysis, Supervision, Resources, Writing - original draft, Writing - review & editing.

Declaration of Competing Interest

The authors report no declarations of interest.

Acknowledgment

The work was financially supported in the Czech Republic through the project of Czech Science Foundation GACR19-21068S and by Operational Programme Research, Development and Education financed by European Structural and Investment Funds and the Czech Ministry of Education, Youth and Sports, partner network CZ.02.1.01/0.0/0.0/17049/0008422, as well as in Poland partly by the National Center for Research and Development (NCBiR) under grant No. 347324/12/NCBR/2017, Materials Technologies project granted by Warsaw University of Technology under the program Excellence Initiative: Research University (ID-UB), and the National Agency for Academic Exchange (NAWA) under grant No. PPN/BIL/2018/1/00126. P. Sezemsky acknowledges the support of University of South Bohemia grant agency by GAJU 110/2020/P project. Authors acknowledge prof. Jan Sterba and his research group for delivering biological material for the biosensing experiment.

References

[1] D. Krohn, T. MacDouglas, A. Mendez, Fibre Optics Sensor: Fundamentals and Applications, 4th ed., SPIE PRESS, Washington, USA, 2014.
[2] S. Yin, P.B. Ruffin, F.T.S. Yu (Eds.), Fiber Optic Sensors, 2nd ed., CRC press, New York, USA, 2008.
[3] S.P. Usha, A.M. Shrivastav, B.D. Gupta, Semiconductor metal oxide/polymer based Fiber optic lossy mode resonance sensors: a contemporary study, Opt. Fib. Technol. 45 (2018) 146–166.
[4] F. Chiavaioli, P. Zubiate, I. Del Villar, C.R. Zamarreño, A. Giannetti, S. Tombelli, C. Trono, F.J. Arregui, I.R. Matias, F. Baldini, Femtomolar detection by nanocoated fiber label-free biosensors, ACS Sens. 3 (5) (2018) 936–943.
[5] I. Del Villar, M. Hernaez, C.R. Zamarreño, P. Sanchez, C. Fernandez-Valdivielso, F. J. Arregui, I.R. Matias, Design rules for lossy mode resonance based sensors, Appl. Opt. 51 (19) (2012) 4298–4307.
[6] N. Paliwal, J. John, Lossy mode resonance based fiber optic sensors, in: I.R. Matias, S. Ikezawa, J. Corres (Eds.), Fiber Optic Sensors: Current Status and Future Possibilities, Vol. 21, Springer International Publishing, Switzerland, 2017.
[7] F. Arregui, I. J.; Del Villar, C.R. Zamarreño, P. Zubiate, I.R. Matias, Giant sensitivity of optical Fiber sensors by means of lossy mode resonance, Sens. Actuat. B 232 (2016) 660–665.
[8] M. Marciniak, J. Grzegorzewski, M. Szustakowski, Analysis of lossy mode cutoff conditions in Planar Wave-Guides with semiconductor guiding layer, IEE Pro.-J. Optoelectron. 140 (4) (1993) 247–252.
[9] A. Andreev, B. Pantchev, P. Danesh, B. Zafirova, E. Karakoleva, E. Vlaikova, E. Alipieva, A refractometric sensor using index-sensitive mode resonance between single-mode Fiber and thin film amorphous silicon waveguide, Sens. Actuat. B 106 (1) (2005) 484–488.
[10] J. Ascorbe, J.M. Corres, I.R. Matias, F.J. Arregui, High sensitivity humidity sensor based on cladding-etched optical Fiber and lossy mode resonances, Sens. Actuat. B 233 (2016) 7–16.
[11] G. Korotcenkov, Metal oxides for solid-state gas sensors: what determines our choice? Mater. Sci. Eng. B 139 (1) (2007) 1–23.
[12] S.P. Usha, B.D. Gupta, Performance analysis of zinc oxide-implemented lossy mode resonance-based optical Fiber refractive index sensor utilizing thin Film/Nanostructure, Appl. Opt. 56 (20) (2017) 5716–5725.
[13] M. Hernaez, I. Del Villar, C.R. Zamarrẽo, F.J. Arregui, I.R. Matias, Optical Fiber refractometers based on lossy mode resonances supported by TiO2 coatings, Appl. Opt. 49 (20) (2010) 3980–3985.
[14] D. Burnat, M. Koba, Ł. Wachnicki, S. Gieraltowska, M. Godlewski, M. Śmietana, Refractive index sensitivity of optical fiber lossy-mode resonance sensors based on atomic layer deposited TiOx thin overlay, in: E. Lewis (Ed.), Sixth European Workshop on Optical Fibre Sensors, Proceedings of 6th European Workshop on Optical Fibre Sensors, Univ. Limerick, Limerick, Ireland, May 31-Jun 03, SPIE-INT SOC Optical Engineering: Bellingham, USA, 2016; 99161G, 2016.
[15] M. Śmietana, M. Dudek, M. Koba, B. Michalak, Influence of diamond-like carbon overlay properties on refractive index sensitivity of nano-coated optical fibres, Phys. Status Solidi A 210 (10) (2013) 2100–2105.
[16] B. Michalak, M. Koba, M. Śmietana, Silicon nitride overlays deposited on optical fibers with RF PECVD method for sensing applications: overlay uniformity aspects, Acta Phys. Pol. A 127 (6) (2015) 1587–1590.
[17] K. Kosiel, M. Koba, M. Masiewicz, M. Śmietana, Tailoring properties of lossy-mode resonance optical Fiber sensors with atomic layer deposition technique, Opt. Laser Technol. 102 (2018) 213–221.
[18] C.R. Zamarreño, P. Zubiate, M. Sagües, I.R. Matias, F.J. Arregui, Experimental demonstration of lossy mode resonance generation for transverse-magnetic and transverse-electric polarizations, Opt. Lett. 38 (14) (2013) 2481–2483.
[19] P.J. Rivero, A. Urrutia, J. Goicoechea, F.J. Arregui, Optical Fiber humidity sensors based on localized surface plasmon resonance (LSPR) and lossy-mode resonance (LMR) in overlays loaded with silver nanoparticles, Sens. Actuat. B 173 (2012) 244–249.
[20] I. Del Villar, C.R. Zamarreño, M. Hernaez, F.J. Arregui, I.R. Matias, Lossy mode resonance generation with indium-tin-Oxide-Coated optical fibers for sensing applications, J. Light. Technol. 28 (1) (2010) 111–117.
[21] T. Minami, Transparent conducting oxide semiconductors for transparent electrodes, Semicond. Sci. Technol. 20 (4) (2005) S35–S44.
[22] A. Socorro, I. B.; Del Villar, J.M. Corres, F.J. Arregui, I.R. Matias, Spectral width reduction in lossy mode resonance-based sensors by means of tapered optical fibre structures, Sens. Actuators B Chem. 200 (2014) 53–60.
[23] L. Razquin, C.R. Zamarreño, F.J. Munoz, I.R. Matias, F.J. Arregui, Thrombin detection by means of an aptamer based sensitive coating fabricated onto LMR-based optical fiber refractometer, in: 2012 IEEE Sens. Proc., Proceedings of the 11th IEEE Sensors Conference, Taipei, TAIWAN, OCT 28-31, IEEE: New York, USA, 2012, 2012, pp. 1104–1107.
[24] J. George, C.S. Menon, Electrical and optical properties of Electron beam evaporated ITO thin films, Surf. Coat. Technol. 132 (1) (2000) 45–48.
[25] J.H. Kim, T.Y. Seong, K.J. Ahn, K.B. Chung, H.J. Seok, H.J. Seo, H.K. Kim, The effects of film thickness on the electrical, optical, and structural properties of cylindrical, rotating, magnetron-sputtered ITO films, App. Surf. Sci. 440 (2018) 1211–1218.
[26] H. Hillebrandt, M. Tanaka, Electrochemical characterization of self-assembled alkylsiloxane monolayers on indium-tin oxide (ITO) semiconductor electrodes, J. Phys. Chem. B 105 (19) (2001) 4270–4276.
[27] X. Jiang, L. Zhang, S.J. Dong, Assemble of poly(Aniline-Co-O-Aminobenzenesulfonic acid) three-dimensional tubal net-works onto ITO electrode and its application for the direct electrochemistry and electrocatalytic behavior of cytochrome C, Electrochem. Commun. 8 (7) (2006) 1137–1141.
[28] S.D. Branch, A.M. Lines, J. Lynch, J.M. Bello, W.R. Heineman, S.A. Bryan, Optically transparent thin-film electrode chip for spectroelectrochemical sensing, Anal. Chem. 89 (14) (2017) 7324–7332.
[29] P. Niedziałkowski, W. Białobrzeska, D. Burnat, P. Sezemsky, V. Stranak, H. Wulff, T. Ossowski, R. Bogdanowicz, M. Koba, M. Śmietana, Electrochemical performance of indium-tin-oxide-coated lossy-mode resonance optical fiber sensor, Sens. Actuators B 301 (2019), 127043.

[30] M. Sobaszek, D. Burnat, P. Sezemsky, V. Stranak, R. Bogdanowicz, M. Koba, K. Siuzdak, M. Śmietana, Enhancing electrochemical properties of an ITO-Coated lossy-mode resonance optical Fiber sensor by electrodeposition of PEDOT:PSS, Opt. Mat. Express 9 (7) (2019) 3069–3078.
[31] M. Śmietana, M. Sobaszek, B. Michalak, P. Niedziałkowski, W. Białobrzeska, M. Koba, P. Sezemsky, V. Stranak, J. Karczewski, T. Ossowski, et al., Optical monitoring of electrochemical processes with ITO-Based lossy-mode resonance optical Fiber sensor applied as an electrode, J. Lightwave Technol. 36 (4) (2018) 954–960.
[32] M. Janik, P. Niedziałkowski, K. Lechowicz, M. Koba, P. Sezemsky, V. Stranak, T. Ossowski, M. Śmietana, Electrochemically directed biofunctionalization of lossy-mode resonance optical fiber sensor, Opt. Express 28 (11) (2020) 15934–15942.
[33] R. Bogdanowicz, P. Niedziałkowski, M. Sobaszek, D. Burnat, W. Białobrzeska, Z. Cebula, P. Sezemsky, M. Koba, V. Stranak, T. Ossowski, et al., Optical detection of ketoprofen by its electropolymerization on an indium tin oxide-coated optical Fiber probe, Sensors 18 (5) (2018) 1361.
[34] M. Śmietana, M. Koba, P. Sezemsky, K. Szot-Karpinska, D. Burnat, V. Stranak, J. Niedziolka-Jonsson, R. Bogdanowicz, Simultaneous optical and electrochemical label-free biosensing with ITO-Coated lossy-mode resonance sensor, Biosens. Bioelectron. 154 (2020), 112050.
[35] A.T. Andreev, B.S. Zafirova, E.I. Karakoleva, A.O. Dikovska, P.A. Atanasov, Highly sensitive refractometers based on a side-polished single-mode fibre coupled with a metal oxide thin-film planar waveguide, J. Opt. A Pure Appl. Opt. 10 (3) (2008), 035303.
[36] S.P. Usha, A.M. Shrivastav, B.D. Gupta, A contemporary approach for design and characterization of fiber-optic-Cortisol sensor tailoring LMR and ZnO/PPY molecularly imprinted film, Biosens. Bioelectron. 87 (2017) 178–186.
[37] I. Del Villar, C.R. Zamarreño, P. Sanchez, M. Hernaez, C.F. Valdivielso, F. J. Arregui, I.R. Matias, Generation of lossy mode resonances by deposition of High-Refractive-Index Coatings on Uncladded Multimode Optical Fibers, J. Opt. 12 (9) (2010), 095503.
[38] A. Ozcariz, C.R. Zamarreño, P. Zubiate, F.J. Arregui, Is there a frontier in sensitivity with lossy mode resonance (LMR) based refractometers? Sci. Rep. 7 (2017) 10280.
[39] I. Del Villar, C.R. Zamarreño, M. Hernaez, P. Sanchez, F.J. Arregui, I.R. Matias, Generation of surface plasmon resonance and lossy mode resonance by thermal treatment of ITO thin-films, Opt. Laser Technol. 69 (2015) 1–7.
[40] X.S. Yin, W. Tang, X.L. Weng, L.J. Deng, Surface morphology modelling for the resistivity analysis of low temperature sputtered indium tin oxide thin films on polymer substrates, J. Phys. D-Appl. Phys. 42 (22) (2009), 225304.
[41] D. Kim, Improvement of structural and optoelectrical properties by post-deposition Electron beam annealing of ITO thin films, Renew. Energy 36 (2) (2011) 525–528.
[42] B. He, H.Z. Wang, Y.G. Li, Z.Q. Ma, J. Xu, Q.H. Zhang, C.R. Wang, H.Z. Xing, L. Zhao, D.D. Wang, Fabrication and characterization of amorphous ITO/p-Si heterojunction solar cell, Sci. China-Technol. Sci. 56 (8) (2013) 1870–1876.
[43] V. Stranak, R. Bogdanowicz, P. Sezemsky, H. Wulff, A. Kruth, M. Śmietana, J. Kratochvil, M. Cada, Z. Hubicka, Towards high quality ITO coatings: the impact of nitrogen admixture in HiPIMS discharges, Surf. Coat. Technol. 335 (2018) 126–133.
[44] K. Ellmer, T. Welzel, Reactive magnetron sputtering of transparent conductive oxide thin films: role of energetic particle (Ion) bombardment, J. Mater. Res. 27 (5) (2012) 765–779.
[45] J.T. Gudmundsson, N. Brenning, D. Lundin, U. Helmersson, High power impulse magnetron sputtering discharge, J. Vac. Sci. Technol. A 30 (3) (2012), 030801.
[46] N. Britun, T. Minea, S. Konstantinidis, R. Snyders, Plasma diagnostics for understanding the plasma-surface interaction in HiPIMS discharges: a review, J. Phys. D Appl. Phys. 47 (22) (2014), 224001.
[47] V. Stranak, A.P. Herrendorf, S. Drache, M. Cada, Z. Hubicka, M. Tichy, R. Hippler, Highly ionized physical vapor deposition plasma source working at very low pressure, Appl. Phys. Lett. 100 (14) (2012), 141604.
[48] B. Finke, M. Polak, F. Hempel, H. Rebl, C. Zietz, V. Stranak, G. Lukowski, R. Hippler, R. Bader, J.B. Nebe, et al., Antimicrobial potential of copper-containing titanium surfaces generated by ion implantation and dual high power impulse magnetron sputtering, Adv. Eng. Mat. 14 (5) (2012) B224–B230.
[49] H. Wulff, H. Steffen, Characterization of thin films, in: 2nd, in: R. Hippler, H. Kersten, M. Schmidt, K.H. Schoenbach (Eds.), Low Temperature Plasmas, Vol. 1, Wiley-VCH, Berlin, Germany, 2008, pp. 375–408.
[50] F.M. Smits, Measurement of sheet resistivities with the 4-Point probe, Bell Syst. Tech. J. 37 (3) (1958) 711–718.
[51] E. Hecht, Optics, 4th ed., Addison Wesley, San Francisco, USA, 2002.
[52] A. Gang, G. Gabernet, L.D. Renner, L. Baraban, G. Cuniberti, A simple two-step silane-based (bio-) receptor molecule immobilization without additional binding site passivation, RSC Adv. 5 (2015) 35631–35634.
[53] M. Janczuk-Richter, B. Gromadzka, Ł. Richter, M. Panasiuk, K. Zimmer, P. Mikulic, W.J. Bock, S. Maćkowski, M. Śmietana, J. Niedziółka Jönsson, Immunosensor based on long-period Fiber gratings for detection of viruses causing gastroenteritis, Sensors 20 (2020) 813.
[54] E. Terzini, P. Thilakan, C. Minarini, Properties of ITO thin films deposited by RF magnetron sputtering at elevated substrate temperature, Mat. Sci. Engin. B 77 (1) (2000) 110–114.
[55] S.D. Senol, A. Senol, O. Ozturk, M. Erdem, Effect of annealing time on the structural, optical and electrical characteristics of DC sputtered ITO thin films, J. Mat. Sci.: Mat. in Elect. 25 (11) (2014) 4992–4999.
[56] S. Kment, P. Kluson, Z. Hubicka, J. Krysa, M. Cada, I. Gregora, A. Deyneka, Z. Remes, H. Zabova, L. Jastrabik, Double hollow cathode plasma jet-low temperature method for the TiO2-xNx photoresponding films, Electrochim. Acta 55 (5) (2010) 1548–1556.
[57] M. Wolcyrz, R. Kubiak, S. Maciejewski, X-ray-Investigation of thermal-expansion and atomic thermal vibrations of tin, indium, and their alloys, Physica Status Solidi B-Basic Res. 107 (1) (1981) 245–253.
[58] M. Quaas, C. Eggs, H. Wulff, Structural studies of ITO thin films with the rietveld method, Thin Solid Films 332 (1–2) (1998) 277–281.
[59] G.B. Gonzalez, J.B. Cohen, J.H. Hwang, T.O. Mason, J.P. Hodges, J.D. Jorgensen, Neutron diffraction study on the defect structure of indium-tin-Oxide, J. Appl. Phys. 89 (5) (2001) 2550–2555.
[60] L. Zhao, Z. Zhou, H. Peng, R. Cui, Indium tin oxide thin films by Bias magnetron RF sputtering for heterojunction solar cells application, Appl. Surf. Sci. 252 (2) (2005) 385–392.
[61] Y.S. Jung, S.S. Lee, Development of indium tin oxide film texture during DC magnetron sputtering deposition, J. Cryst. Growth 259 (4) (2003) 343–351.
[62] K.S. Tseng, Y.L. Lo, Effect of sputtering parameters on optical and electrical properties of ITO films on PET substrates, Appl. Surf. Sci. 285 (2013) 157–166.
[63] G. Frank, H. Köstlin, Electrical-properties and defect model of tin-doped indium oxide layers, Appl. Phys. A Mat. Sci. Proc. 27 (4) (1982) 197–206.
[64] M. Huang, Z. Hameiri, A.G. Aberle, T. Mueller, Influence of discharge power and annealing temperature on the properties of indium tin oxide thin films prepared by Pulsed-DC magnetron sputtering, Vacuum 121 (2015) 187–193.
[65] A. Sytchkova, D. Zola, L.R. Bailey, B. Mackenzie, G. Proudfoot, M. Tian, A. Ulyashin, Depth dependent properties of ITO thin films grown by pulsed DC sputtering, Mater. Sci. Eng. B. 178 (9) (2013) 586–592.
[66] R.L. McCreery, Advanced carbon electrode materials for molecular electrochemistry, Chem. Rev. 108 (7) (2008) 2646–2687.
[67] N. Kurapati, P. Pathirathna, Ch.J. Ziegler, S. Amemiya, Adsorption and electron-transfer mechanisms of ferrocene carboxylates and sulfonates at highly oriented pyrolytic graphite, ChemElectroChem 6 (22) (2019) 5651–5660.
[68] C.S. Fang, K.H. Oh, A. Oh, K. Lee, S. Park, S. Kim, J.K. Park, H. Yang, An Ultrasensitive and Incubation-Free Electrochemical Immunosensor Using a Gold-Nanocatalyst Label Mediating Outer-Sphere-Reaction-Philic and Inner-Sphere-Reaction-Philic Species, Chem. Commun. 52 (34) (2016) 5884–5887.
[69] R.W. French, A.M. Collins, F. Marken, Growth and application of paired gold electrode junctions: evidence for nitrosonium phosphate during nitric oxide oxidation, Electroanalysis 20 (22) (2008) 2403–2409.
[70] M. Śmietana, P. Niedziałkowski, W. Białobrzeska, D. Burnat, P. Sezemsky, M. Koba, V. Stranak, K. Siuzdak, T. Ossowski, R. Bogdanowicz, Study on combined optical and electrochemical analysis using indium-tin-Oxide-Coated optical Fiber, Electroanalysis 31 (2) (2019) 398–404.
[71] I. Del Villar, F.J. Arregui, C.R. Zamarreño, J.M. Corres, C. Bariain, J. Goicoechea, C. Elosua, M. Hernaez, P.J. Rivero, A.B. Socorro, et al., Optical sensors based on lossy-mode resonances, Sens. Actua. B Chemical 240 (2017) 174–185.
[72] N.D. Popovich, S.-S. Wong, B.K.H. Yen, H.-Y. Yeom, D.C. Paine, Influence of microstructure on the electrochemical performance of tin-doped indium oxide film electrodes, Anal. Chem. 74 (13) (2002) 3127–3133.
[73] M.A. Martínez, J. Herrero, M.T. Gutiérrez, Electrochemical stability of indium tin oxide thin films, Electrochim. Acta 37 (14) (1992) 2565–2571.
[74] T. Sannomiya, H. Dermutz, C. Hafner, J. Vörös, A.B. Dahlin, Electrochemistry on a localized surface plasmon resonance sensor, Langmuir 26 (10) (2010) 7619–7626.
[75] J.H. Ghithan, M. Moreno, G. Sombrio, R. Chauhan, M.G. O'Toole, S.B. Mendes, Influenza virus immunosensor with an electro-active optical waveguide under potential modulation, Opt. Lett. 42 (7) (2017) 1205–1208.
[76] J. Juan-Colás, A. Parkin, K.E. Dunn, M.G. Scullion, T.F. Krauss, S.D. Johnson, The electrophotonic silicon biosensor, Nat. Commun. 7 (2016) 12769.

Petr Sezemsky is a Ph.D. student at the University of South Bohemia in branch of Biophysics. His work is focused on research and deposition of bioactive and biofunctional surfaces. His field of interest is low-temperature plasma deposition, bio-functional and antibacterial surfaces, sensor technique.

Dariusz Burnat received a B.Sc. and M.Sc. degree from Warsaw University of Technology, Poland, in 2015 and 2018, respectively. Currently, he is working towards a Ph.D. degree in the Institute of Microelectronics and Optoelectronics, Warsaw University of Technology. His research interests include sputtered thin films for optical fiber sensors.

Jiri Kratochvil received his Ph.D. in Biophysics, Chemical and Macromolecular Physics at Charles University, Czech Republic in 2020. His scientific focus is materials science, nanoparticles and surface engineering, their characterization and application in biomedicine and biochemistry, i.e. antimicrobial coatings, surfaces with tailored wettability, surfaces for nanoparticle enhanced bio-detection methods.

Harm Wulff received a Ph.D. in Physical Chemistry at the University of Greifswald. 1988 he qualified as a university lecturer and received the Venia Legendi for Physical Chemistry. From 1993–2003 he was project leader in the SFB 198 "Kinetics of partial ionized plasmas" funded by the German Research Foundation and from 2004 to 2009 project leader in the Transregional Collaborative Research Centre 24 "Fundamentals of Complex Plasmas "(German Research Foundation). His field of interest are surface layers in reactive plasmas.

Angela Kruth studied Chemistry at University of Greifswald, Germany, and obtained her PhD from University of Aberdeen, U.K, in solid state chemistry. Main research activities are new materials for energy applications, such as electroceramics and metal-carbon hybrids. At the Leibniz Institute of Plasma Science and Technology in Greifswald, she is head of the Materials for Energy Technologies group.

Katarzyna Lechowicz received a B.Sc. degree from Warsaw University of Technology, Poland in 2019. Currently, he is working towards a M.Sc. degree in the Institute of Microelectronics and Optoelectronics, Warsaw University of Technology. His research interests include transparent oxides for optical fiber and electrochemical sensors.

Monika Janik received the B.Sc. and M.Sc. degrees in biotechnology from the Wroclaw University of Science and Technology, Poland, in 2014 and 2015, respectively. In 2019 she received a Ph.D. degree in photonics from the Université du Québec en Outaouais, Canada. Her current interests include designing and optimizing different kinds of biosensors.

Robert Bogdanowicz received his Ph.D. degree (with distinction) in Electronics from the Gdansk University of Technology in 2009. His current domains of interest include selective CVD diamond growth and nanocrystalline diamond doping for environmental and biochemical nanosensors. In 2015 he held a scholarship Fulbright Senior Scholar Program at the California Institute of Technology (Caltech) in the group of prof. William Goddard (Materials and Process Simulation Center) working on hybrid 3D diamond structures.

Martin Cada received his M.Sc. and Ph.D. in plasma physics from the Charles University in Prague, Czech Republic in years 2000 and 2004, respectively. Afterwards he spent two years as a postdoctoral fellow at the University of Liverpool (UK) in group of Prof. J. W. Bradley. Since 1998 he is employed at the Institute of Physics of Czech Academy of Sciences as a senior researcher. His research interests include low-temperature plasma diagnostics and PVD deposition of functional thin films.

Zdenek Hubicka graduated from Charles University Faculty Mathematics and Physics, where he obtained also PhD degree in 1998. Since 2000 he works in the Institute of Physics CAS Prague Czech Republic like researcher and he leads The Department of Low-Temperature Plasma since 2006. His research interest are low temperature plasma, PVD and PECVD thin films deposition and plasma diagnostics.

Paweł Niedziałkowski received a M.Sc. and Ph.D. (with distinction) degrees in chemistry from the University of Gdansk, Poland, in 2004 and 2010, respectively. His main research interests include organic synthesis of supramolecular compounds, as well as modification and characterization of different type of electrode surface to make them more sensitive towards selected analytes.

Wioleta Białobrzeska received her M.Sc. degree from the University of Gdańsk, Poland, in 2015. Currently, she is working towards a Ph.D. degree in the Department of Supramolecular Chemistry, University of Gdansk. Her research interests include electrochemical measurements, especially the examination of interaction of organic compounds with oxygen and with DNA.

Vitezslav Stranak received a Ph.D. from the Charles University in Prague, Czech Republic in 2007. Afterwards he was a postdoctoral fellow in Greifswald (Germany) oriented on low-temperature plasma diagnostics and deposition of thin film. Since 2013 he is with University of South Bohemia, Czech Republic as associated professor performing applied research of thin nanostructured and functional thin films.

Mateusz Śmietana received his B.Sc., M.Sc., Ph.D. (with distinction), and D.Sc. degrees in electronics from the Warsaw University of Technology (WUT), Poland, in 2000, 2002, 2007, and 2014, respectively. Since December 2015, he has been an Associate Professor in the Institute of Microelectronics and Optoelectronics, WUT. He was a postdoctoral fellow at Virginia Tech, USA and Université du Québec en Outaouais, Canada, as well as a visiting professor at Southern University of Science and Technology (China). He has authored and co-authored more than 150 scientific papers. His fields of interest are fiber-optic sensors and thin films.